

# New techniques for measuring and modeling cavern dimensions in a Bingham plastic fluid

R.J. Wilkens\*, J.D. Miller, J.R. Plummer, D.C. Dietz, K.J. Myers

Department of Chemical and Materials Engineering, School of Engineering, University of Dayton, Dayton, Ohio 45469, USA

Received 10 September 2004; received in revised form 17 March 2005; accepted 5 April 2005

Available online 15 June 2005

## Abstract

A model for predicting the mixing cavern dimensions for Bingham plastic fluids based on the assumption of equal torque is developed. Experimental data has been collected for the purpose of verifying this model, using a novel technique, for both axial and radial flow impellers in a tank of Heinz ketchup. The mixing caverns were found to be the shape of an elliptical torus. The ellipse aspect ratios were determined for both impeller types and are assumed to be constant. The model was able to predict the cavern diameter and cavern height within the experimental uncertainty.

© 2005 Elsevier Ltd. All rights reserved.

*Keywords:* Cavern diameter prediction; Cavern diameter measurement; Complex fluids; Fluid mechanics; Mixing; Non-Newtonian fluids; Rheology

## 1. Introduction and literature review

Understanding agitation mechanisms is critical to industrial scale-up. Newtonian agitation is well understood. In non-Newtonian agitation, however, available models are often insufficient to use for scale-up (Wilkens et al., 2003).

During agitation of highly shear-thinning and Bingham plastic fluids in a mixing tank it is common to generate an agitated volume, a cavern near the impeller, and an unagitated volume, where the fluid in the remainder of the mixing tank is stagnant. Understanding these caverns is an important component of agitation design. While all fluids have the potential for regions of good and poor mixing, these particular non-Newtonian fluids often have regions of no fluid motion, therefore poor mixing by definition.

Fig. 1 defines how these fluid types perform, i.e., the shear stress ( $\tau_{yx}$ ), at various shear rates ( $dv_x/dy$ ). A Newtonian fluid has a linear relationship between the shear stress

and the shear rate and which also passes through the origin. A non-Newtonian fluid is any fluid that deviates from this behavior. A shear-thinning, or pseudo-plastic, fluid is a type of non-Newtonian fluid in which the slope of the shear stress decreases with increasing shear rate. A yield stress, or Bingham plastic, fluid is a type of non-Newtonian fluid in which the shear stress does not pass through the origin. That is, a minimum shear stress, i.e., the yield stress, must be reached before any velocity gradient can occur. Thus, the yield stress,  $\tau_0$ , is the minimum shear stress required to allow fluid motion.

The slopes of the curves shown in Fig. 1 give the apparent viscosities,  $\mu_a$ , of the fluids:

$$\mu_a = \frac{d(-\tau_{yx})}{d\left(\frac{dv_x}{dy}\right)} \quad (1)$$

For a Newtonian fluid,  $\mu_a = \mu$ :

$$-\tau_{yx} = \mu \frac{dv_x}{dy} \quad (2)$$

\* Corresponding author. Tel.: +1 937 229 2627.

E-mail address: wilkens@udayton.edu (R.J. Wilkens).

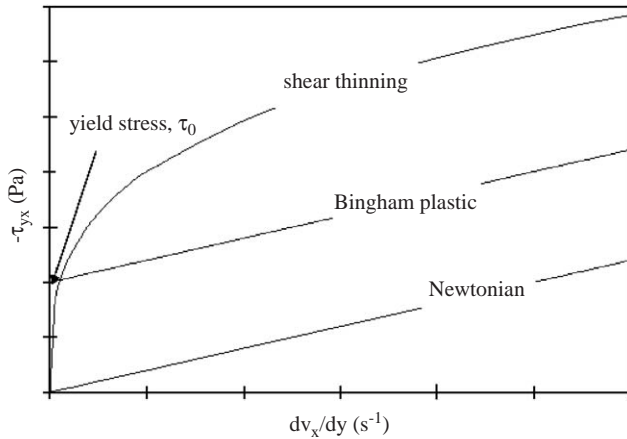


Fig. 1. Shear stress diagram in Cartesian coordinates with only an  $x$  velocity component.

For a shear-thinning fluid, the performance is often represented using a power-law relationship:

$$-\tau_{yx} = K' \left( \frac{dv_x}{dy} \right)^{n'} \quad (3)$$

$$\mu_a = n' K' \left( \frac{dv_x}{dy} \right)^{n'-1} \quad (4)$$

For a yield stress fluid,  $\mu_a \rightarrow \infty$  ( $-\tau_{yx} < \tau_0$ ) or  $\mu_a = \mu_p$  ( $\tau_{yx} \geq \tau_0$ ):

$$-\tau_{yx} = \tau_0 + \mu_p \frac{dv_x}{dy} \quad (5)$$

The effective viscosity,  $\mu_{\text{eff}}$ , is the ratio of the shear stress to the shear rate and is used in determining the impeller Reynolds number:

$$Re = \frac{\rho N D^2}{\mu_{\text{eff}}} \quad (6)$$

For a shear-thinning fluid:

$$\mu_{\text{eff}} = K' \left( \frac{dv_x}{dy} \right)^{n'-1} \quad (7)$$

Paul et al. (2004), suggest that for a yield stress fluid:

$$\mu_{\text{eff}} = \frac{\tau_0 + \mu_p \frac{dv_x}{dy}}{\frac{dv_x}{dy}} \approx \frac{\tau_0}{\frac{dv_x}{dy}} \quad (8)$$

For a mixing tank the shear rate can be replaced with the effective shear rate, given by:

$$\left( \frac{dv_x}{dy} \right)_{\text{eff}} = k_s N \quad (9)$$

For the impellers used in this study the effective shear rate constant,  $k_s$ , is 11 (Bakker and Gates, 1995).

When analyzing the agitation of a non-Newtonian fluid presenting shear-thinning or Bingham plastic characteristics, there are several ways of modeling the flow characteristics. One such way is to determine the characteristic cavern diameter. The cavern is defined as a region in which the fluid is being mixed or agitated. Outside of this cavern the fluid is stagnant. In the case of a Bingham Plastic fluid, the cavern is comprised of the region where the shear stress is greater than the fluid's yield stress. The size of the cavern is dependent upon fluid properties, impeller characteristics, and the rotational speed and torque of the impeller.

Solomon et al. (1981) proposed predicting the cavern in a yield stress fluid based on a torque balance. They suggested that the cavern was spherical and that at the cavern boundary the shear stress was equal to the yield stress. From this they were able to develop a model to predict the cavern diameter.

Other models used alternative shapes to the spherical cavern. Some extended the results to highly shear thinning fluids. Amanullah et al. (1998) reviewed previous cavern diameter modeling attempts and proposed a model for highly shear-thinning fluids assuming a toroidal cavern.

In an opaque material, such as ketchup, it is difficult to obtain visual confirmation of the mixing cavern leading to the need of expensive laboratory equipment such as an X-ray machine. This paper proposes a novel experimental approach to the problem of determining the mixed cavern dimensions in an opaque material by injecting glitter, freezing the fluid, and dissecting the frozen solid. A model is also presented to predict the cavern dimensions generated by two different impeller types.

## 2. Model development

A model for determining the cavern size has been developed that is based on the assumption that the boundary is defined by the yield stress of the fluid. That is, the rotational energy is dissipated at the cavern boundary regardless of the direction of the velocity gradient. This leads to a rotational drag force of

$$F = \tau_0 A_c \quad (10)$$

$A_c$  is the surface area of the mixing cavern. Since the force is applied over a range of radial positions, it is best to consider the torque:

$$M = F R_{\text{eq}} \quad (11)$$

$R_{\text{eq}}$  is the equivalent radius. It represents the average radial position where the force is applied. This is also the torque imparted by the impeller on the fluid. This does not include the axial component of force, if present, as discussed later.

Researchers and modelers have found the shape of the mixing cavern to be best represented as a torus (Amanullah et al., 1998; Galindo and Nienow, 1992). This assumption will be discussed with the experimental results. Fig. 2

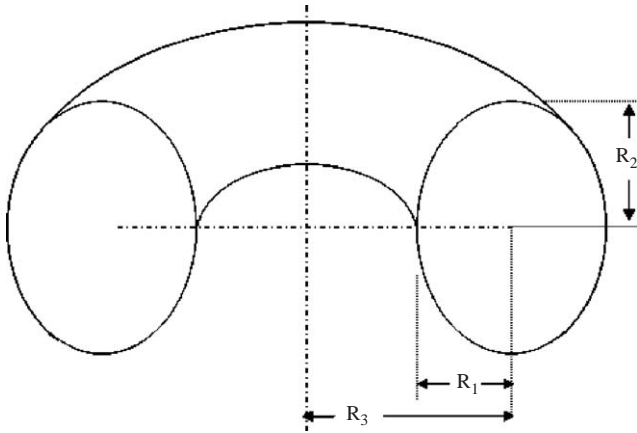


Fig. 2. Elliptical torus general shape and associated dimensions.

illustrates an elliptical torus. Assuming the ellipse cross-section to be taller than it is wide,  $R_1$  is the minor axis radius of the ellipse and  $R_2$  is the major axis radius. The distance from the center of the ellipse to the axis of rotation is indicated by  $R_3$ .

The surface area of the torus is thus determined from

$$A_c = 2\pi R_3 P_c. \quad (12)$$

The perimeter of a slice of the cavern is indicated by  $P_c$ . Calculation of  $P_c$  is non-trivial. First consider  $\beta$ , the ratio of major to minor axis ( $R_2/R_1$ ). For the range of  $\beta$  expected in the mixing caverns ( $1 < \beta < 3$ ), the Ramanujan second approximation for the perimeter of the ellipse, as shown by Bourke (2004), is recommended (valid for  $\beta < 22$ ):

$$P_c = \pi(R_2 + R_1) \left[ 1 + \frac{3 \left( \frac{R_2 - R_1}{R_2 + R_1} \right)^2}{10 + \left( 4 - 3 \left( \frac{R_2 - R_1}{R_2 + R_1} \right)^2 \right)^{1/2}} \right]. \quad (13)$$

This expression can be restated by introducing a new variable,  $\alpha$ , which is only a function of  $\beta$ .

$$P_c = \alpha\pi R_1, \quad (14)$$

where

$$\alpha = (\beta + 1) \left[ 1 + \frac{3 \left( \frac{\beta - 1}{\beta + 1} \right)^2}{10 + \left( 4 - 3 \left( \frac{\beta - 1}{\beta + 1} \right)^2 \right)^{1/2}} \right]. \quad (15)$$

If the center of the torus is closed, as suggested by Amanullah et al. (1998), then  $R_3 = R_1$  as shown in Fig. 3. Revisiting the equivalent radius for the torque imparted, symmetry can be assumed. For every point above the minor axis there is a point below the minor axis. That is, the ellipse is symmetric about the impeller location

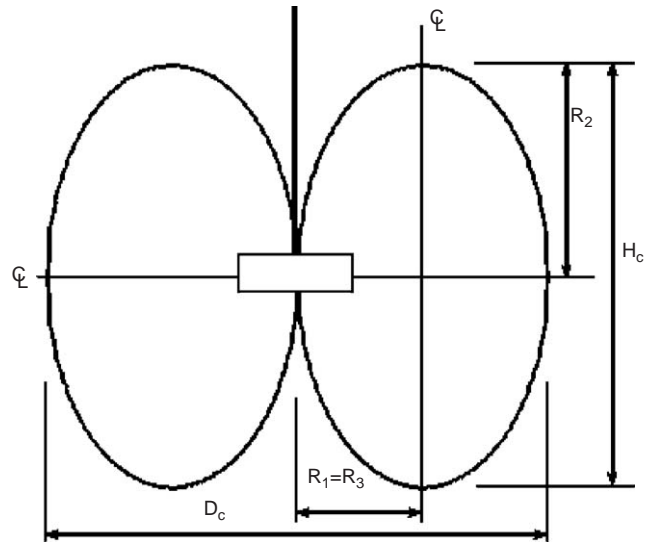


Fig. 3. Cross-sectional view of elliptical torus mixing cavern.

(axial direction). Likewise, a symmetry argument can be used to say that the ellipse is symmetric in the radial direction. To a first approximation then, the average radial position of the force,  $R_{eq}$ , can be estimated to be  $R_1$ . Thus the torque imparted to the fluid is given by

$$M = 2\pi^2 \alpha \tau_0 R_1^3. \quad (16)$$

From this, the mixing cavern diameter and height can be determined from

$$D_c = 4R_1 = \left( \frac{32M}{\pi^2 \alpha \tau_0} \right)^{1/3}, \quad (17)$$

$$H_c = \frac{\beta D_c}{2}. \quad (18)$$

These relationships should be used with caution as they are not bound by vessel size. It is assumed in this model that the torque due to the yield stress at the cavern boundary equals the torque imparted by the impeller to the fluid. The torque imparted by the impeller is either known by measurement or is predicted at the design stage using the power number:

$$M = \frac{N_P \rho N^2 D^5}{2\pi}. \quad (19)$$

These equations can also be rearranged to determine the torque for a given cavern diameter or the speed for a given cavern diameter. The implication is that the torque imparted by the impeller equals the torque dissipated at the cavern boundary. This assumption will be addressed in the results and discussion.

### 3. Materials and methods

A Bench Scale Equipment ELB experimental agitator (manufactured by Chemineer, Inc.) was used to conduct the



Fig. 4. Photograph of the straight and pitched impellers used in the study.



Fig. 5. Example of cavern diameter for ketchup with top exposed (the baffles are not necessary).

mixing operations. A  $\frac{1}{4}$ -hp motor was mounted vertically with a variable speed gearbox, allowing shaft speeds of up to 800 rpm. Two impeller types were used: a flat six-blade impeller for the study of radial flow, a six-blade impeller pitched at  $45^\circ$  for the study of axial flow. Fig. 4 shows the two different impeller types. The blade width to impeller diameter ratio ( $W/D$ ) was constant at  $\frac{1}{8}$ . The impeller diameters used were 2.5" (0.0634 m) and 3.0" (0.0762 m) for radial flow and 2.5" for axial flow.

Rotational speed was measured using a hand-held tachometer (Omega). The agitator drive is supported by a thrust bearing. Attached to the drive base is an arm connected to a force gauge (Ametek). This allows for the measurement of torque imparted to the fluid.

Heinz ketchup was selected as the fluid to be agitated. Fig. 5 demonstrates the cavern formation in a baffled tank. A region in the center of the tank is mixed while the outer region is not in motion. A clear division can be seen between these two regions. The division indicates the location of the yield stress. Heinz ketchup has a density of  $1160 \text{ kg/m}^3$ . The yield stress was determined to be 15 Pa (Brookfield viscometer).

The ketchup was only filled slightly above the impeller for the photograph of Fig. 5. If the liquid level was sufficiently high, a cavern would still form but would not be visible. To combat this obstacle a novel approach was used to establish the mixing cavern.

The cavern size is determined in a baffle-free mixing tank. Baffles are not necessary as the flow is expected to be laminar in the cavern and the boundary is stagnant process fluid. Vessel size is not of critical importance. The higher the rotational speed the larger the cavern diameter. Once the cavern diameter reaches the vessel wall the shape of the cavern will become distorted, thus all experiments will be conducted below this maximum rotational speed for the given tank size.

The rotational speed at which the cavern boundary reaches the wall can be readily found if the tank is clear (i.e., wall motion is observed). If there is no top or bottom motion, then this is the maximum rotational speed for the tank.

Once a maximum rotational speed is established, two slower speeds are also selected, and three colors of glitter are chosen to correspond to the three mixing speeds. The motor is set just below the maximum rotational speed for the tank and the power is turned off. A highly concentrated mixture of glitter in ketchup is injected at the impeller. The motor is turned on and the ketchup is then mixed at the high speed for approximately 15 min to ensure complete mixing.

The motor speed is then adjusted down to the second speed. The motor is again turned off and a different color of glitter is injected. The process is repeated for all desired conditions. The assumption is that the glitter is small enough to not affect the hydrodynamics. It is also assumed that no significant settling will occur. Thus, the location of the glitter represents only the region mixed at the specified rotational speed.

When the mixing is completed the tank is placed in a large freezer for several days. After freezing, the ketchup is ready to be dissected for examination of the cavernous regions. First, the ketchup is cut away from the walls of the container using a saw blade as shown in Fig. 6. Next, a cut is made through the center of the frozen sample. The sample is then cut in half again, allowing one quarter of the original sample to be removed by hand. In this process one quarter of the sample will be destroyed, one quarter will be examined, and one half will be preserved for further analysis if necessary. Care must be taken not to disturb the second quarter while removing the first.

With the first quarter removed, the second quarter can be carefully removed in one piece to allow for a detailed inspection of the mixing patterns, represented by the distributions of each glitter color. Glitter pieces that have been smeared on the exposed face from dissection process must be distinguished from those that are actually frozen into the ketchup. The cavern shape can then be traced on the surface of the sample, as shown in Fig. 7, and the dimensions of the mixing region can then be measured.

#### 4. Results and discussion

The method of freezing the ketchup was a success. The shape of the mixing cavern, for both impeller types, was found to be an elliptical torus as expected. This can be seen in



Fig. 6. Cutting and removal of the frozen ketchup.

Table 1  
Flow region and impeller dimensions for experimental data

Impeller type	$D$ (m)	$D_c/2$ (m)	$H_c$ (m)	$N$ (rot/s)	$M$ (Nm)	$\beta$
Straight	0.0762	0.105	0.164	12.5	0.102	1.56
Straight	0.0762	0.075	0.103	8.33	0.040	1.37
Straight	0.0634	0.070	0.125	10.0	0.045	1.79
Straight	0.0634	0.045	0.070	7.50	0.011	1.56
Pitched	0.0634	0.065	0.150	7.50	0.023	2.31

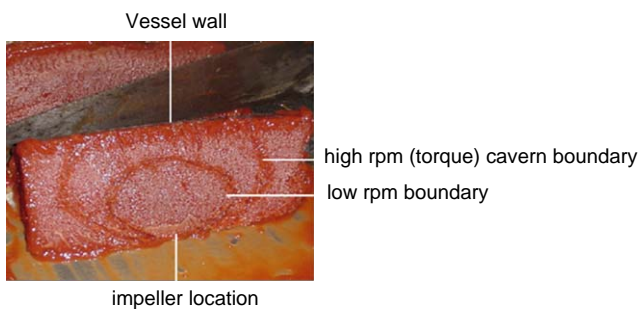


Fig. 7. The sample of frozen ketchup to be investigated. The edge of the glitter regions were scored into the frozen ketchup. The two regions shown represent different rotational speeds for the same impeller type and diameter.

the photograph shown in Fig. 7. A summary of the measured parameters is listed in Table 1.

$\beta$  increased slightly as the rotational speed was increased. The slight increase could be due to interactions with the mixing tank wall at the higher rotational speeds. It was expected that the ratio would be relatively constant for a given impeller type. The average value for  $\beta$  for the straight blade impeller was found to be 1.6. The value for the pitched blade impeller was 2.3. This means that the cavern for a pitched blade impeller is taller than that of a radial impeller at equal cavern diameter. This increase was expected due to the nature of the flow patterns for the two types of impellers.

The measured cavern diameter was found to increase with increasing rotational speed. This was expected since more energy is imparted to the fluid at higher rotational speeds. For the radial flow impeller, impeller diameter had no apparent effect on the cavern diameter at equal torque. Only one valid

data point was collected for the axial flow impeller as the higher rotational speeds led to significant interaction with the mixing tank bottom.

Others have suggested that the axial thrust must be included when modeling the cavern diameter (Amanullah et al., 1998). For a radial flow impeller there is no axial thrust. For a system of this size, the axial thrust component of the axial flow impeller is not expected to be significant. Its exclusion makes the cavern diameter prediction accurate for the straight blade impeller and conservative (underestimate cavern size) for the pitched blade impeller.

The resulting values of  $\alpha$  are 2.3 (radial flow impeller) and 3.4 (axial flow impeller). Thus the cavern dimensions for the radial flow impeller are:

$$D_c = 1.08 \left( \frac{M}{\tau_0} \right)^{1/3}, \quad (20)$$

$$H_c = 0.85 \left( \frac{M}{\tau_0} \right)^{1/3}. \quad (21)$$

For the axial flow impeller the model is reduced to:

$$D_c = 0.98 \left( \frac{M}{\tau_0} \right)^{1/3}, \quad (22)$$

$$H_c = 1.13 \left( \frac{M}{\tau_0} \right)^{1/3}. \quad (23)$$

Note that there is only a small change in the cavern diameter coefficient despite a significant difference in the ratio  $\beta$ . This is because  $D_c$  is a weak function of  $\beta$ . An error of  $\beta$  being 1.5 instead of 1.6 only introduces a 1% change in the

Table 2  
Model comparison for ketchup results ( $\tau_0 = 15$  Pa)

Impeller type	$D$ (m)	$N$ (rot/s)	$M$ (N m)	$Re$	$D_c$ (m) measured	$D_c$ (m) model	$H_c$ (m) measured	$H_c$ (m) model
Straight	0.0762	12.5	0.102	810	0.21	0.20	0.16	0.16
Straight	0.0762	8.33	0.040	540	0.15	0.15	0.10	0.12
Straight	0.0634	10.0	0.045	540	0.14	0.16	0.12	0.12
Straight	0.0634	7.50	0.011	400	0.09	0.10	0.07	0.08
Pitched	0.0634	7.50	0.023	400	0.13	0.11	0.15	0.13

Table 3  
Comparison to selected data from Amanullah et al. (1998), tank ID = 0.45 m, SCABA 3SHP1 impeller ( $\tau_0 = 4$  Pa)

$N$ (rot/s)	$M$ (N m) measured	$D_c$ (m) measured	$D_c$ (m) predicted Amanullah model	$D_c$ (m) new model
0.250	0.005	0.15	0.11	0.11
0.333	0.005	0.16	0.12	0.13
0.583	0.009	0.19	0.17	0.14
0.833	0.011	0.20	0.19	0.16
1.250	0.016	0.22	0.24	0.17
1.667	0.022	0.26	0.29	0.19
2.083	0.028	0.30	0.32	0.20
2.500	0.035	0.33	0.38	0.23
2.917	0.050	0.45	0.43	0.25

predicted cavern diameter. The predicted cavern height is more sensitive to the term  $\beta$  because of a one-to-one relationship.

Table 2 summarizes the measured cavern diameter and the predicted cavern diameter. The model results for the cavern diameter and cavern height are within uncertainty of the measured cavern dimensions. The prediction for the axial flow impeller is slightly conservative, as expected. The model predicts no impeller diameter effect for equal torque. Other models were investigated but none were directly applicable to this system. Their application led to poor predictions and the results are not worth reporting here.

Table 3 is a comparison of the new model to the data of Amanullah et al. (1998). A yield stress of 4 Pa was assumed for this highly shear-thinning fluid based on the rheological performance plot in the paper. The model prediction is good at low rotational speeds where the axial force is not significant. It under-predicts cavern diameter at higher speeds where the axial force begins to dominate the rotational force, as expected.

## 5. Conclusions

A new technique was established for determining the cavern dimensions of an opaque Bingham plastic fluid. A simplified constant torque model was shown to be able to predict the cavern diameter within the uncertainty of the measurement. The only parameters needed to determine the characteristics of the flow region for the new model are the

impeller type, torque of the impeller system, and yield stress of the fluid. The impeller type determines the aspect ratio,  $\beta$ , of the elliptical torus. The aspect ratios of a six blade radial impeller and a six blade pitched impeller were determined.

Further investigations will demonstrate the repeatability of the aspect ratios observed for these systems and the influence of impeller diameter on torque. Determining and confirming characteristic aspect ratios for various impellers could expand the applications of this model. The advantages of this model are its simplicity and accuracy. The disadvantages of this model are the need of knowing the aspect ratio a priori (although only a minor affect on cavern diameter) and the need for accurate power number data for mixing the cavern (e.g., simply replace known  $D/T$  corrections with  $D/D_c$ ?) to predict the torque requirement.

It is recommended that this model be used for radial flow impellers and for axial flow impellers only when the axial force is negligible.

## Notation

$A_c$	cavern surface area, m <sup>2</sup>
$D$	impeller diameter, m
$D_c$	cavern diameter, m
$F$	force, N
$H_c$	cavern height, m
$k_s$	effective shear rate constant, dimensionless
$K'$	flow consistency coefficient of a power law fluid, Pa s <sup><math>n'</math></sup>
$M$	torque, N m
$n'$	flow behavior index of a power law fluid, dimensionless
$N$	rotational speed, rot s <sup>-1</sup>
$N_P$	power number, dimensionless
$P_c$	cavern perimeter, m
$R_1$	ellipse minor axis radius, m
$R_2$	ellipse major axis radius, m
$R_3$	radial distance to center of ellipse from center of torus, m
$R_{eq}$	equivalent radius, m
$Re$	impeller Reynolds number, dimensionless
$v_x$	velocity in $x$ direction, m
$T$	tank diameter, m
$W$	impeller blade width, m

### Greek letters

$\alpha$	ellipse parameter, dimensionless
$\beta$	ratio of ellipse major axis to minor axis, dimensionless
$\mu$	fluid viscosity, Pa s
$\mu_a$	apparent fluid viscosity, Pa s
$\mu_{\text{eff}}$	effective fluid viscosity, Pa s
$\mu_p$	plastic viscosity, Pa s
$\rho$	fluid density, kg m <sup>-3</sup>
$\tau_0$	fluid yield stress, Pa
$\tau_{yx}$	shear stress, Pa

### Acknowledgements

The authors acknowledge ReyNo Inc (<http://www.reynoinc.com>) for the mixing software license and support.

### References

- Amanullah, A., Hjorth, S.A., Nienow, A.W., 1998. A new mathematical model to predict cavern diameters in highly shear thinning power law liquids using axial flow impellers. *Chemical Engineering Science* 53, 455–469.
- Bakker, A., Gates, L.E., 1995. Properly choose mechanical agitators for viscous liquids. *Chemical Engineering Progress* 91, 25–34.
- Bourke, P., 2004. Circumference of an ellipse. <http://astronomy.swin.edu.au/~pbourke/geometry/ellipsecirc/>.
- Galindo, E., Nienow, A.W., 1992. Mixing of highly viscous simulated Xanthan fermentation broths with the Lightnin A315 impeller. *Biotechnology Progress* 8, 233–239.
- Paul, E.L., Atiemo-Obeng, V.A., Kresta, S.M., 2004. *Handbook of Industrial Mixing*. Wiley, New York.
- Solomon, J., Elson, T.P., Nienow, A.W., Pace, G.W., 1981. Cavern sizes in agitated fluids with a yield stress. *Chemical Engineering Communications* 11, 143–164.
- Wilkens, R.J., Henry, C., Gates, L.E., 2003. How to scale-up mixing processes in non-Newtonian fluids. *Chemical Engineering Progress* 99, 44–49.